ELSEVIER

Thin Solid Films 273 (1996) 143–148

thin solid films

Local elasticity measurement on polymers using atomic force microscopy

H.-Y. Nie [a,*], M. Motomatsu [b], W. Mizutani [a], H. Tokumoto [a]

[a] *Joint Research Center for Atom Technology, National Institute for Advanced Interdisciplinary Research, Higashi 1-1-4, Tsukuba, Ibaraki 305, Japan*

[b] *Joint Research Center for Atom Technology, Angstrom Technology Partnership, Higashi 1-1-4, Tsukuba, Ibaraki 305, Japan*

Abstract

Local elasticity was measured on polymers by modifying atomic force microscopy (AFM) in which the sample height was modulated and the response of the cantilever was detected. In a case of polystyrene (PS) on mica, there existed many circular holes in the film that were stiffer than the rest parts. The holes were identified as the substrate mica surface and the rest as PS films. In the case of a polyethyleneoxide surface on mica, a crystalline nature was observed. In addition, the surface was modified by scanning an AFM tip at large forces of 20 nN. The scanned area exhibited an increase in elasticity as well as formation of a striped structure.

Keywords: Atomic force microscopy; Polymers; Electrical properties and measurements; Surface morphology

1. Introduction

Atomic force microscopy (AFM) has been developed as a powerful tool to image surface features of materials. An important feature from the AFM images is a surface topography that is obtained by keeping forces between the surface and tip constant with the usage of a relatively soft cantilever. In addition to the topographic feature, we can probe local elastic properties of materials through a mechanical interaction between the surface and tip [1–7]. This interaction is detected by indenting the sample surface with the AFM tip [3–5], during which a force–distance curve is measured. When the force–distance curve is analyzed by the Hertzian model [8] by assuming an appropriate geometry of the tip apex, Young's modulus can be deduced. To do this type of measurements, a method called force modulation microscopy was developed, where both images reflecting elasticity distribution and topographic nature were obtained simultaneously [9,10]. We used this technique to map the elasticity of polystyrene (PS) on mica and evaluate their Young's moduli by fitting the force–distance curve to the Hertzian model.

Recently, there has been increasing interest in modifying the surface locally using the AFM tip. Among various modifications, we shall concentrate on the one induced by mechanical forces between the tip and polymer surface [11,12]. A typical example of this type of modifications is a bundle formation on polyacetylene with large forces [12]. We report here a modification of both the elasticity and surface morphology on crystallized polyethyleneoxide (PEO) surfaces on a nanometer scale.

2. Experiment and method to deduce Young's modulus

2.1. Experiment

We used a commercial AFM system (SPA300, Seiko Instruments Inc.) that was equipped with a quadrant photodetector for detecting the deflection and torsion of the cantilever to obtain topographic and friction force images. Two types of cantilever were used in this study. The stiffer one was a rectangular shaped silicon cantilever with a spring constant of 18 N m^{-1} and a resonance frequency of 236 kHz (Nanoprobe). This cantilever was 3.5, 25 and 138 μm in thickness, width and length, respectively. The length of the tip was 15 μm and the radius of the tip apex was about 20 nm. The torsional spring constant was about 780 N m^{-1}. The softer one was a rectangular shaped silicon cantilever with a spring constant of 0.75 N m^{-1} and a resonance frequency of 88 kHz (Olympus Opt. Inc.). The cantilever was 0.8, 40 and 100 μm in thickness, width and length, respectively. The length of the tip was 2.8 μm and the radius of the tip apex was about 20 nm. In this study we measured the PS on mica and PEO on mica films with the stiffer and softer cantilevers, respectively.

* Corresponding author at: Analytical Sciences Laboratory, Yokohama Research Centre, Mitsubishi Chemical Corporation, 1000 Kamoshida-cho, Aoba-ku, Yokohama 227, Japan. Tel: +81 45 963 3867, Fax: +81 45 963 3974.

SSDI 0040-6090(95)06807-4

The oscillation of the sample height was realized by applying sinusoidal voltage from a function generator to the Z direction of the piezo (PZT) scanner on which the sample was fixed. A 5 kHz sinusoidal voltage, which was higher than the feedback loop frequency of 0.5 kHz but lower than the resonance frequency of the cantilever, was applied to the piezo scanner to oscillate the sample height with a peak-to-peak amplitude of about 1 nm. The response of the cantilever to this oscillation was detected with a lock-in amplifier and was used to obtain images relevant to local elasticity of sample surface. Here we notice that an oscillation of the sample height would not influence topographic images as far as its frequency is higher than the cutoff frequency of the feedback loop. Therefore, we can obtain both topography and elasticity distribution images simultaneously.

Two samples were prepared by spin-coating PS and PEO solutions in benzene onto cleaved mica surfaces. The PS sample was dried at 170 °C in air for 3 h. To prepare a crystallized sample of PEO, it is necessary to anneal the sample at a temperature above the PEO's melting temperature of 66 °C in a moderate vacuum. Therefore, we selected to anneal the PEO sample at 90 °C for 24 h. The sample thickness was about 100 and 200 nm for PS and PEO, respectively. All measurements were carried out in air with a humidity of about 60%. The time constant of the lock-in amplifier was set to 1 ms. An image consisted of 256×256 pixel points and the acquisition time for 1 frame was 8.5 min (i.e. a scan rate of 0.5 Hz).

2.2. *Method to deduce Young's modulus*

Here we apply the Hertzian model to deduce Young's modulus from the measured force–distance curve. Let h be the movement of the piezo scanner stage on which a sample is set, p the deflection of the cantilever beam and d the deformed depth of the sample surface. Then it is obvious that

$$h = p + d \tag{1}$$

The force F applied on the sample as a result of the cantilever deflection, p, is given by the Hooke's law for the cantilever,

$$F = k_c p \tag{2}$$

where k_c is the spring constant of the cantilever.

We can write Eq. (2) as a function of h

$$F(h) = k_c[h - d(h)] \tag{3}$$

Following the Hertzian model, the penetration depth $d(h)$ can be written as [8]

$$d(h) = F(h)^{2/3}(D^2/R)^{1/3} \tag{4}$$

where R is the radius of the tip apex, and D is related to Young's modulus E and Poission's ratio σ in a form of $D = 3(1-\sigma^2)/(4E)$, provided that the Young's modulus of the tip is much larger than that of the sample. Substituting Eq. (4) for Eq. (3), we obtain the relation of the applied force $F(h)$ with the stage movement h as follows:

$$F(h) = k_c[h - F(h)^{2/3}(D^2/R)^{1/3}] \tag{5}$$

This equation is used to fit the measured force–distance curve in our AFM system and to deduce Young's modulus by assuming relevant values for σ, R and k_c.

3. Results and discussion

3.1. *PS on mica*

Typical AFM and simultaneously recorded elasticity images of PS on mica are shown in Fig. 1(a) and 1(b), respectively. In the topographic image (Fig. 1(a)), there

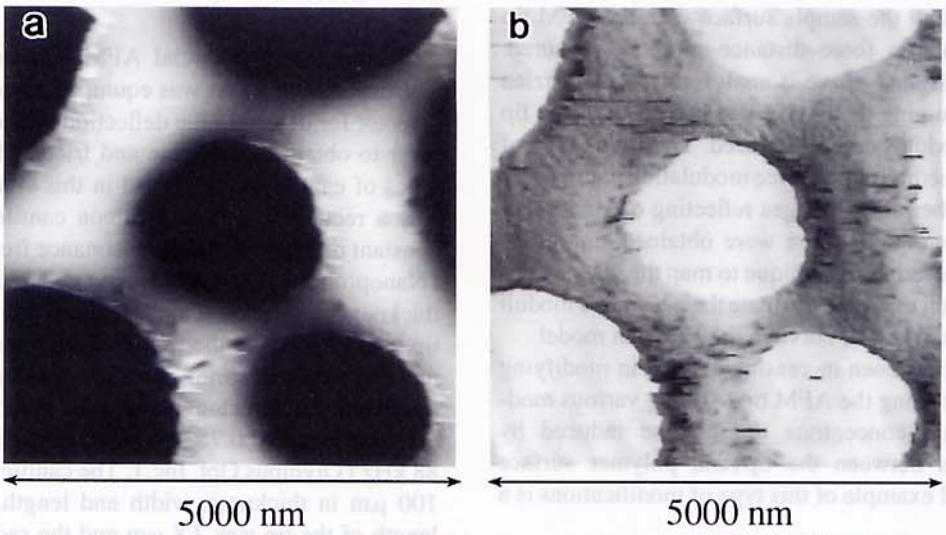

Fig. 1. Topographic (a) and elasticity (b) images of PS on mica obtained simultaneously in an area of 5 000×5 000 nm², with a cantilever whose spring constant was 18 N m^{-1} at a repulsive force of 120 nN. The topography in (a) shows films with average thickness of 25–90 nm and with holes in diameter of 2 000–3 000 nm, respectively. The data in (b) was a direct record of the response of the cantilever to the oscillation of the sample height at 5 kHz with a peak-to-peak amplitude of about 1 nm.

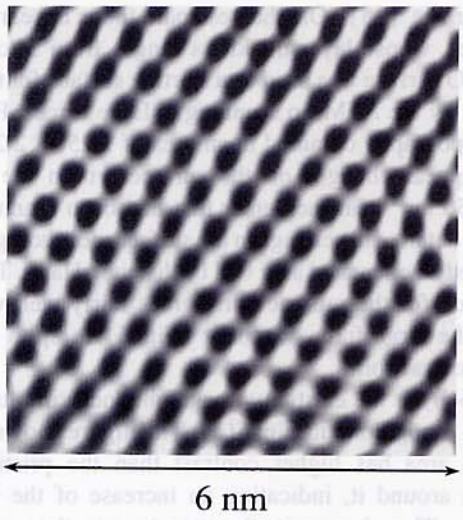

Fig. 2. Atomic resolution image in an area of 6 × 6 nm² obtained with friction force mode at the bottom of a particular hole. A soft cantilever with a spring constant 0.75 N m^{-1} was used. The acquisition time for this friction force image was 16 s.

appear holes with diameters of 2000–3000 nm. The contrast in the elasticity image (Fig. 1(b)) reflects the elasticity distribution in such a way that the brighter expresses the stiffer. There appear circular protrusions with the same diameters and positions as the holes in the topographic image (Fig. 1(a)). Assuming that the elastic properties of the surfaces are the same as those of the bulk ones for both mica and PS, i.e. 172 GPa for mica [13] and 3.4 GPa for PS [14], we can conclude that mica is much stiffer than PS. Then we can identify the holes and rest parts as the mica surface and PS film, respectively.

We also verified this identification by observing atomic images on the hole parts. Fig. 2 shows a friction force image for the surface of holes. The distance between white dots is about 0.54 nm that corresponds to that of mica surfaces. On the parts other than holes, no atomic images were obtained. Therefore, the holes in the topography are assigned to the mica substrate.

Fig. 3(a) shows the force–distance curves measured on PS and mica surfaces and Fig. 3(b) the simultaneously obtained response of the cantilever to the oscillation of the sample height. In these figures, the origin in the horizontal axis is taken at a position where the approaching force goes to zero from attractive to repulsive force. The minus (plus) direction represents approaching (separating) the sample into (from) the tip. Fig. 3(a) shows that the slope of the force–distance curve is larger on mica than on PS. This difference in slope is also seen in Fig. 3(b) and is the origin of the contrast in Fig. 1(b). To evaluate the difference of elasticity between the two surfaces, we shall estimate their Young's moduli by fitting curves after hard contact between the tip and sample to Eq. (5). With assumptions of the tip radius of 20 nm and a Poisson's ratio of 0.33, the Young's moduli are deduced as about 200 and 5 GPa for mica and for PS, respectively. These values are comparable with those of their bulk elastic properties in the literature [13,14].

We also measured the torsion of the cantilever to check whether it influences the normal deflection during the elasticity measurement. The result of the normal deflection and the torsion of the cantilever on mica is plotted in Fig. 4, in which the largest deflection of the cantilever corresponds to a force of about 300 nN. The signals in the figure are direct records from the simultaneous outputs of the quadrant photodetector corresponding to the normal and torsional motions of the cantilever. The vertical line in the figure is a guide for the cantilever deflection without torsion. Noting that a scale for the vertical (deflection) axis is 10 times larger than that for the lateral (torsion) one, the angle between the guide line and the data plot is found to be about 4.5°, resulting in an error of 8% for the deflection. This small error indicates that the effect of the torsion to the deflection is negligible under normal forces up to about 300 nN. In the present experiments,

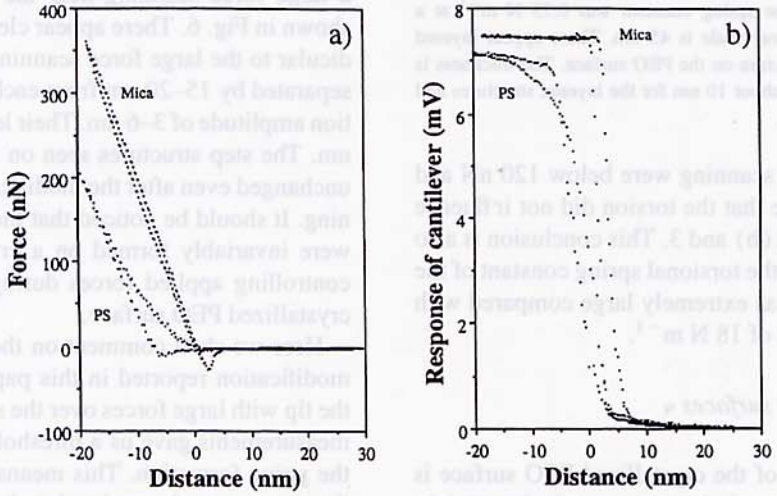

Fig. 3. Force–distance curves (a) and the simultaneous cantilever's responses (b) to the oscillation of the sample height at 5 kHz with a peak-to-peak amplitude of about 1 nm measured on both mica and PS. The same cantilever for Fig. 1 with a spring constant of 18 N m^{-1} was used. The speed of the cantilever to approach toward and to separate from the sample surface was 3 nm s^{-1}.

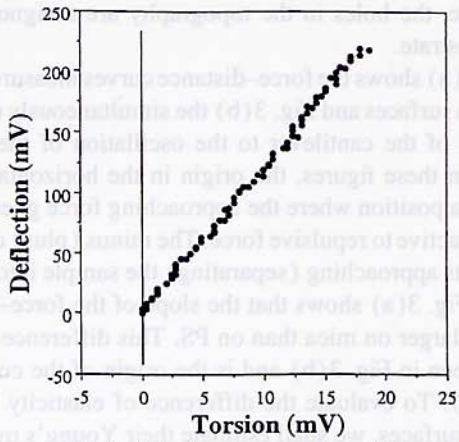

Fig. 4. The curve of the deflection versus torsion of the cantilever when indenting mica surface with a spring constant of 18 N m^{-1}. The data were direct records from the photodetector's outputs. The vertical line is a guide for the cantilever deflection without torsion. The angle between the data and the line appears to be about 4.5°. Note the lateral (torsion) axis is expanded 10 times.

Fig. 5. A typical AFM image of 2 250 × 2 250 nm^2 of the crystallized PEO surface, with a cantilever whose spring constant was 0.75 N m^{-1} at a repulsive force of 6 nN. The gray scale is 45 nm. There appear layered structures over and a spiral structure on the PEO surface. The thickness is in the range of 5–10 nm and is about 10 nm for the layered structures and the spiral structure, respectively.

the average forces during scanning were below 120 nN and therefore we can conclude that the torsion did not influence the results shown in Fig. 1(b) and 3. This conclusion is also supported by the fact that the torsional spring constant of the cantilever, 780 N m^{-1}, was extremely large compared with its normal spring constant of 18 N m^{-1}.

3.2. Modification of PEO surfaces

A typical AFM image of the crystallized PEO surface is shown in Fig. 5. There is a spiral structure at the lower right corner whose layer thickness is about 10 nm, similar to the reported values of the spiral structures on the crystallized PEO surface [15]. On the rest part there appear layered structures, whose layer thickness ranges from 5 to 10 nm. This PEO surface was used as a starting surface for the modification by the AFM tip scanning at large forces. Fig. 6(a) is the topography obtained in an area of 2 250 × 2 250 nm^2. There appear changes on the surface within the area of 750 × 750 nm^2 near the center that had been scanned at 20 nN. The detail of the change in the surface morphology within the large force scanned area will be discussed later. The overall feature for the pristine part agrees fairly well with that before the large force scanning (Fig. 5) in spite of small image contraction.

Fig. 6(b) is the elasticity image obtained simultaneously with the topography in Fig. 6(a). This figure shows that the scanned area has higher contrast than the pristine PEO surfaces around it, indicating an increase of the Young's modulus. The change in the structure is thus obviously accompanied by a change in the elasticity. In order to make a quantitative estimation of the elasticity on the modified area, we measured several force–distance curves both on the modified and the pristine PEO surfaces. Fig. 7 shows typical force–distance curves. The slope of the force–distance curve on the modified area is steeper than that on the pristine parts of PEO. We monitored the torsion of the cantilever during the measurement of force–distance curves and found that the "cross-talk" effect was only a few percentages. Fitting these curves to the Hertzian model by assuming the tip radius of 20 nm and a Poisson's ratio of 0.33, Young's modulus on the modified area is found to increase to 3.5 GPa from 0.3 GPa on the pristine PEO surface. These values of Young's moduli for the pristine and modified PEO surfaces are consistent with those obtained on two other PEO samples and the PEO component of PS-PEO blend films [11]. Although the increase of Young's modulus on the modified PEO surface is surely originated from the deformation of the PEO layers, its mechanism is not clear at this moment.

Fig. 8 shows an AFM image of the modified surface after a large force scanning near the central area of the image shown in Fig. 6. There appear clearly regular stripes perpendicular to the large force scanning direction. The stripes are separated by 15–20 nm from each other and have a corrugation amplitude of 3–6 nm. Their lengths range from 50 to 100 nm. The step structures seen on the pristine parts remained unchanged even after the modification under the 20 nN scanning. It should be noticed that the stripes as shown in Fig. 8 were invariably formed on a crystallized PEO surface by controlling applied forces during scanning, not on a non-crystallized PEO surface.

Here we shall comment on the origin of the stripes. The modification reported in this paper is realized by scanning the tip with large forces over the sample surface. Preliminary measurements gave us a threshold force of about 10 nN for the stripe formation. This means that under applied forces, the tip presses the molecular chains and pushes simultaneously them toward the scanning direction. When the force exceeds the threshold force, the molecular chains start to

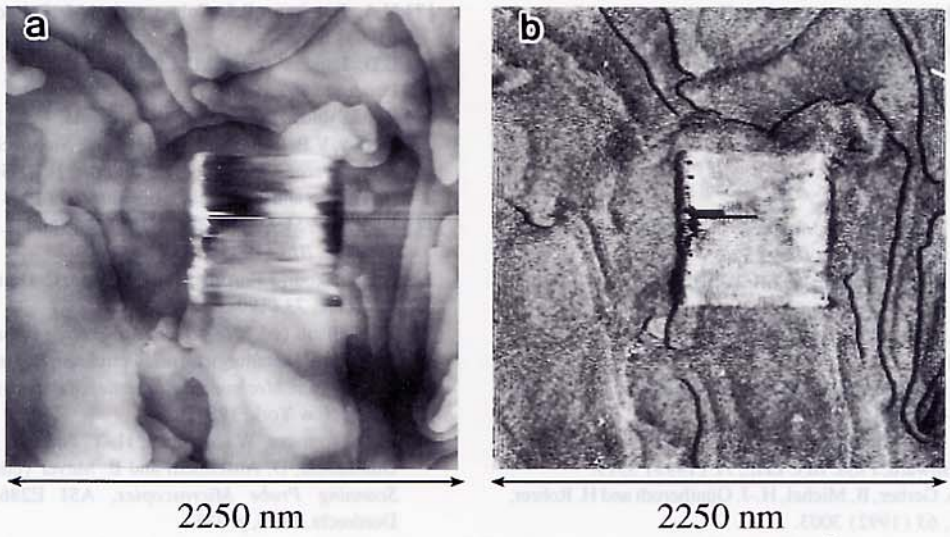

Fig. 6. Simultaneously obtained topographic (a) and elasticity (b) images of PEO surfaces in an area of 2 250×2 250 nm^2 including a central area of 750×750 nm^2 that experienced a large force scanning at 20 nN. The cantilever used was 0.75 N m^{-1} in spring constant and the images were obtained at a repulsive force of 6 nN. The gray scale for (a) is 42 nm. There appear changes both in surface structure and elasticity as seen in the topographic and elasticity images, respectively. The data in (b) was a direct record of the response of the cantilever to the oscillation of the sample height at 5 kHz with a peak-to-peak amplitude of about 1 nm.

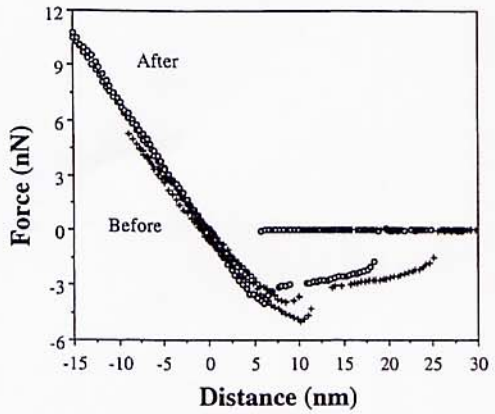

Fig. 7. Force–distance curves measured on the striped area (after the large force scanning and indicated by the circle) and pristine PEO surface (before the large force scanning and indicated by the cross) with a cantilever whose spring constant was 0.75 N m^{-1}. The speed for the tip to approach toward and to separate from the sample surface was 10 nm s^{-1}.

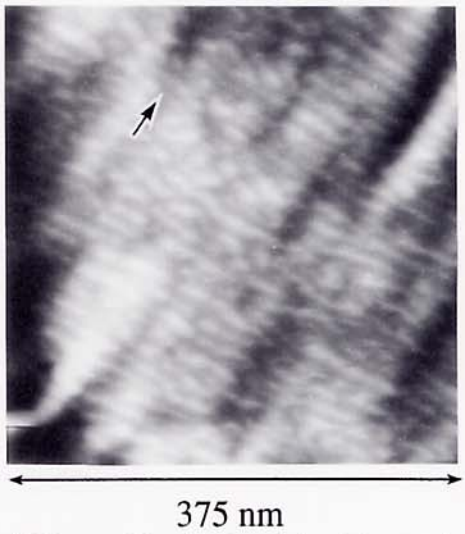

Fig. 8. An AFM image of the striped area induced after scanning the tip at 20 nN in a direction indicated by an arrow. The image was obtained at 6 nN with a cantilever whose spring constant was 0.75 N m^{-1}. The scan area is 375×375 nm^2 and gray scale is 41 nm.

deform plastically. The formation of the stripes is thus considered a result of a balance among the pressure of the tip applied to the sample surface, lateral forces due to the scanning, and strains of the deformed molecular chains.

4. Conclusions

We applied the force modulation technique to map the elasticity distribution of PS on mica and evaluated their Young's moduli by fitting the force–distance curves to the Hertzian model. The surface elasticity of PS on mica was imaged together with the topography, showing that the surface of mica was stiffer than that of PS. Their Young's moduli were evaluated to be about 200 and 5 GPa, close to their bulk elastic properties.

We also used the AFM to modify both surface structure and the local elasticity of PEO crystal. A stripe structure was formed as a result of the deformation of the molecular chains by the large force scanning of the AFM tip. This deformation also caused an increase in Young's modulus. In order to elucidate the real mechanism of this deformation, more precise measurements on, for example, the threshold force, the stress distribution inward the film, and effects of the molecular weight, are highly required.

Acknowledgements

One of the authors (HYN) acknowledges a fellowship supported by the Research Development Corporation of

Japan (JRDC). This work was partially supported by the New Energy and Industrial Technology Development Organization (NEDO).

References

[1] D. Tománek, G. Overney, H. Miyazaki, S.D. Mahanti and H.-J. Güntherodt, *Phys. Rev. Lett., 63* (1989) 876.
[2] S.P. Jarvis, A. Oral, T.P. Weihs and J.B. Pethica, *Rev. Sci. Instrum., 64* (1993) 3515.
[3] D.M. Schaefer, A. Patil, R.P. Andres and R. Reifenberger, *Appl. Phys. Lett., 63* (1993) 1492.
[4] A.L. Weisenhorn, M. Khorsandi, S. Kasas, V. Gotzos and H.-J. Butt, *Nanotechnology, 4* (1993) 106.
[5] P. Tangyunyong, R.C. Thomas, J.E. Houston, T.A. Michalske, R.M. Crooks and A.J. Howard, *Phys. Rev. Lett., 71* (1993) 3319.
[6] D. Anselmetti, Ch. Gerber, B, Michel, H.-J. Güntherodt and H. Rohrer, *Rev. Sci. Instrum., 63* (1992) 3003.
[7] N.A. Burnham, R.J. Colton and H.M. Pollock, *Nanotechnology,* (1993) 64.
[8] L.D. Landau and E.M. Lifshitz, *Theory of Elasticity*, Pergamon London, 1959, p. 30.
[9] P. Maivald, H.-J. Butt, S.A.C. Gould, C.B. Prater, B. Drake, J.A Gurley, V.B. Elings and P.K. Hansma, *Nanotechnology, 2* (1991) 103
[10] R.M. Overney, E. Meyer, J. Frommer, H.-J. Güntherodt, M. Fujihira H. Takano and Y. Gotoh, *Langmuir, 10* (1994) 1281.
[11] H.-Y. Nie, M. Motomatsu, W. Mizutani and H. Tokumoto, *J. Vac. Sci Technol., B13* (1995) 1163.
[12] Z. Elkaakour, J.P. Aimé, T. Bouhacina, C. Odin and T. Masuda, *Phys Rev. Lett., 73* (1994) 3231.
[13] J.L. Gillson (ed.), *Industrial Mineral and Rocks*, American Institut of Mining, Metallurgical, and Petroleum Engineering, 1960, p. 551.
[14] L.E. Nielsen, *Mechanical Properties of Polymers*, Reinhold Publishin Corp., New York, 1967, p. 7.
[15] M. Motomatsu, W. Mizutani, H.-Y. Nie and H. Tokumoto, in H.-J Güntherodt, D. Anselmetti and E. Meyer (eds.), *Proc. of Forces i Scanning Probe Microscopies*, ASI E286, Kluwer Academic Dordrecht, 1995, p. 331.